ACCP
AMERICAN COLLEGE OF CLINICAL PHARMACOLOGY
Advancing Clinical Care through Pharmacology

Population Pharmacokinetic Analysis of BMS-986166, a Novel Selective Sphingosine-1-Phosphate-1 Receptor Modulator, and Exposure-Response Assessment of Lymphocyte Counts and Heart Rate in Healthy Participants

Sébastien Bihorel[1], Shalabh Singhal[2], Diane Shevell[2], Huadong Sun[3], Jenny Xie[2], Shenita Basdeo[2], Ang Liu[2], Santanu Dutta[2], Elizabeth Ludwig[1], Hannah Huang[1], Kuan-ju Lin[4], Aberra Fura[2], John Throup[2], and Ihab G. Girgis[2]

Abstract

Sphingosine-1-phosphate (S1P) binding to the S1P-1 receptor (S1P1R) controls the egress of lymphocytes from lymphoid organs and targets modulation of immune responses in autoimmune diseases. Pharmacologic modulation of S1P receptors has been linked to heart rate reduction. BMS-986166, a prodrug of the active phosphorylated metabolite BMS-986166-P, presents an improved cardiac safety profile in preclinical studies compared to other S1P1R modulators. The pharmacokinetics, safety, and pharmacodynamics of BMS-986166 versus placebo after single (0.75–5.0 mg) and repeated (0.25–1.5 mg/day) oral administration were assessed in healthy participants after a 1-day lead-in placebo period. A population model was developed to jointly describe BMS-986166 and BMS-986166-P pharmacokinetics and predict individual exposures. Inhibitory sigmoid models described the relationships between average daily BMS-986166-P concentrations and nadir of time-matched (day −1) placebo-corrected heart rate on day 1 (nDDHR, where DD represents $\Delta\Delta$) and nadir of absolute lymphocyte count (nALC). Predicted decreases in nDDHR and nALC were 9 bpm and 20% following placebo, with maximum decreases of 10 bpm in nDDHR due to drug effect, and approximately 80% in nALC due to drug and placebo. A 0.5-mg/day dose regimen achieves the target 65% reduction in nALC associated with a 2-bpm decrease in nDDHR over placebo.

Keywords

ALC, BMS-986166, heart rate, PK/PD, S1P1R

Sphingosine-1-phosphate (S1P) is a bioactive lysophospholipid that mediates a variety of cellular responses by the stimulation of the G-protein–coupled S1P receptors (S1PRs) 1,2,3,4,5 (S1P1-5R)[1,2] present on a wide range of human cells and tissues. The sphingosine-1-phosphate-1 receptor (S1P1R) subtype is expressed on the surface of lymphocytes and is important in regulating egress of T cells and B cells from peripheral lymph nodes.[3] The S1PR modulators indirectly antagonize the function of this receptor, leading to sequestration of lymphocytes in the lymph nodes.[4] Based on this pharmacologic effect, functional interference with S1P1R has been targeted as a mechanism to diminish inappropriate immune responses and modulate autoimmune diseases.

In 2010, fingolimod (Gilenya) was approved by the US Food and Drug Administration[5] for the

[1]Cognigen Corporation, a *SimulationsPlus* Company, Buffalo, New York, USA

[2]Bristol Myers Squibb, Princeton, New Jersey, USA

[3]Previously employed at Bristol Myers Squibb, Princeton, New Jersey, USA

[4]Previously employed at Cognigen Corporation, a *SimulationPlus* Company, Buffalo, New York, USA

Corresponding Author:
Ihab G. Girgis, MSc, PhD, 3401 Princeton Pike, Lawrenceville, NJ 08648, USA
(e-mail: ihab.girgis@bms.com)

treatment of relapsing-remitting multiple sclerosis. As an unselective agonist of S1PRs and as a selective functional antagonist of the S1P1 subtype by induction of receptor downregulation,[5] fingolimod is associated with several safety concerns including bradycardia, atrioventricular block, increased blood pressure, and macular edema.[6] In particular, the slowing of heart rate (HR) results from S1P binding to multiple receptors, including S1P1R.[7,8] A range of effect on HR reduction has been observed in humans treated with various S1P1R modulators, including amiselimod,[9,10] cenerimod,[11] ceralifimod,[12] GSK2018682,[13] ozanimod,[14] ponesimod,[15,16] and siponimod.[17,18] These results indicate that slowing of HR in humans is related to differential effects on the S1P1R activity by these modulators. More importantly, the range of effects exhibited by this class of compounds suggests that there is a potential for a discovery of an S1P1R modulator with minimal effects on HR.

BMS-986166[2] is a small-molecule S1P1R modulator currently under development for the treatment of various autoimmune diseases, including ulcerative colitis. BMS-986166 is orally administered as a prodrug that undergoes phosphorylation into its active metabolite BMS-986166-P (BMT-121795). Unlike the phosphorylated metabolite of fingolimod, fingolimod-P, which is a full S1P1R agonist, BMS-986166-P was shown to be a partial S1P1R agonist. It was further demonstrated that this differentiated S1P1R pharmacology reduced the risk for cardiovascular and pulmonary liability and macular edema compared to fingolimod, at doses that maintain comparable reduction in lymphocyte counts and efficacy in animal models of multiple sclerosis, inflammatory bowel disease, and systemic lupus erythematosus (in-house data).

In vitro data suggest that while BMS-986166 is metabolized via cytochrome P450 (CYP) 3A4/3A5 ($\sim$68%) and CYP2C8 ($\sim$36%), it was not a reversible or time-dependent inhibitor of CYP1A2, CYP2B6, CYP2C8, CYP2C9, CYP2C19, CYP2D6, or CYP3A4 and uridine diphosphate glucuronosyltransferase 1A1 at the anticipated therapeutic doses. In cryopreserved human hepatocytes, BMS-986166 was not an inducer of CYP1A2, CYP2B6, or CYP3A4. In vitro studies indicate that BMS-986166 is not an inhibitor of various human efflux and uptake drug transporters including P-glycoprotein, breast cancer resistance protein, organic anion transporting polypeptide B1, organic anion transporting polypeptide B3, bile salt export pump, organic anion transporter 1, organic anion transporter 3, sodium taurocholate cotransporting polypeptide, or multidrug resistance–associated protein 2. Overall, the present results indicate that the potential for BMS-986166 as a perpetrator of drug-drug interactions is minimal.

Systemic plasma exposure (maximum plasma concentration and area under the curve from time 0 to 24 hours) of BMS-986166 and BMS-986166-P in healthy subjects were approximately dose proportional over the range of 0.75 to 5 mg with single doses, and over 0.25 to 1.5 mg multiple doses.[19] Median time of peak concentration across all dose levels occurred between 9.0 and 15.0 hours for BMS-986166 and between 6.0 and 9.0 hours for BMS-986166-P after multiple doses. The apparent terminal elimination half-life ranged from 276 to 321 hours for BMS-986166 and from 270 to 304 hours for BMS-986166-P.

This report describes the pharmacokinetic (PK) and pharmacodynamic (PD) behavior of BMS-986166 or BMS-986166-P in humans as characterized using a modeling and simulation approach. A population PK (PPK) model for both BMS-986166 and BMS-986166-P was developed to provide exposures for quantitative relationships between BMS-986166-P exposures and reduction in absolute lymphocyte counts (ALCs) and HR following single and repeated fixed dosing in healthy participants. Finally, model simulations were used to predict BMS-986166-P PK exposures, HR, and ALC responses to guide dose selection for phase 2 clinical trial design and to achieve an optimal therapeutic benefit/safety balance.

Methods

Study Design

Two double-blinded, placebo-controlled, randomized clinical trials using a single-ascending dose design (Study IM018001)[20] and a multiple-ascending dose design (Study IM018003)[21] were conducted to assess the safety and tolerability of BMS-986166 after oral administration of a liquid formulation in healthy participants. In both studies, subjects were admitted to a clinic facility on day 2 for completion of screening assessments. A single dose of placebo was administered to all subjects during the lead-in phase on day −1, 24 hours ahead of the randomized placebo or active treatment dose. Subjects underwent baseline exams including predose serial 12-lead electrocardiograms (ECGs) (predose [0 hours], 2, 4, 8, and 12 hours), telemetry monitoring, and continuous cardiac monitoring with an external monitoring device, as well as serial CBC (complete blood counts) with that included ALC (predose [0 hours], 3, 6, 9, 12, 15, and 18 hours) during this lead-in period.

In Study IM018001, subjects were randomized to receive BMS-986166 as a single dose of 0.75, 2.0, or 5.0 mg (n = 10/group; 4:1 ratio of BMS-986166:placebo) on day 1. Blood samples were intensively collected for determination of plasma concentrations of BMS-986166 and BMS-986166-P

and ALC from before dosing to 816 hours after dosing, as detailed in Table S1. Subjects were monitored by telemetry starting on day -1 through 24 hours after dosing on day 1. Data from continuous cardiac monitoring using an external monitoring device was obtained from 24 hours before and up to 72 hours after dosing and used for detailed assessment of HR changes. Standard ECGs were assessed at periodic intervals using 12-lead ECG. Subjects remained in the clinic for 6 days after dosing and were furloughed after clinical and laboratory assessments were completed on day 7. Subjects returned to the clinic for safety, PK, and PD assessments on days 10, 14, 21, 28, and 35. Subjects enrolled in the relative bioavailability/food effect part of the single-ascending dose study were not included in the PK or PD analyses.

In Study IM018003, BMS-986166 was administered as once-daily doses of 0.25 mg (n = 12; 2:1 ratio of BMS-986166:placebo) and 0.75 mg or 1.5 mg (n = 10/dose; 4:1 ratio of BMS-986166:placebo). Blood samples for determination of plasma concentrations of BMS-986166 and BMS-986166-P and ALC were collected in most groups before and after dosing with an intense sampling schedule after the 1st, 14th, and 28th doses. Continuous HR monitoring with an external monitoring device was performed from 24 hours before and up to 72 hours after the 1st dose, and from before and up to 24 hours after the 14th dose. In both studies, the HR measurements performed on day 1 after subjects received a placebo dose allowed for the intraindividual correction of HR measurements collected at later time intervals.

Both clinical trials were performed at PPD Development, LLC (Austin, Texas), in accordance with good clinical practice guidelines and under the guiding principles of the Declaration of Helsinki. Before enrollment, all participants were informed about the risks of the studies and signed an informed consent form. All study protocols and consent forms were reviewed and approved by the institutional review board of Integreview (Austin, Texas) and by the US Food and Drug Administration as appropriate.

Bioanalytical Methods
BMS-986166 and BMS-986166-P concentrations were measured in blood lysate using a validated liquid chromatography–mass spectrometry (MS) assay. The concentration range of the assay was 0.100 ng/mL to 100 ng/mL for both compounds. Samples for analyses were prepared by protein precipitation followed by liquid-liquid extraction. Chromatographic separation was performed on a reversed-phase C18 column (Acquity UPLC BEH C18 column) followed by positive-ion electrospray ionization and MS/MS detection. The chromatographic mobile phase used was a mix of 0.1%

formic acid in water and 0.1% formic acid in acetonitrile. The method utilized $^{13}C_6$-BMS-986166 and $^{13}C_6$-BMT-121795 as internal standards and monitored a mass-to-charge ratio of 345 for both BMS-986166 and BMT-121795 and 351 for both internal standards. For BMS-986166, $\leq$4.9 coefficient of variation expressed as a percent (%CV) was observed for between-day variability and $\leq$7.2 %CV was observed for within-day variability. For BMT-121795, $\leq$9.8 %CV was observed for between-day variability and $\leq$5.8 %CV was observed for within-day variability.

Analysis Software
NONMEM Version 7.3.0 (ICON Development Solutions, Dublin, Ireland) was used for nonlinear mixed-effects modeling with the first-order conditional estimation method with interaction.[22] Tabular and graphical data displays were created with KIWI Version 2.0 (Cognigen Corporation, Buffalo, New York)[23] and SAS version 9.4 (SAS Institute, Cary, North Carolina).[24] Summary statistics calculated from observed and simulated data (eg, the 5th, 50th, and 95th percentiles of the distributions of concentration) used in creation of visual predictive check plots were generated with Perl-Speaks-NONMEM Version 4.4.0.[25]

Pharmacokinetic and Exposure-Response Model Development
Various linear and nonlinear structural models were explored to characterize the PPK of both BMS-986166 and BMS-986166-P. A sequential approach was applied to first identify a suitable PK model for BMS-986166 using the pooled data from both studies. In a combined model for BMS-986166 and BMS-986166-P PK, the PK parameters as well as random variability in these parameters for BMS-986166 were then fixed to the population (typical value) estimates and BMS-986166-P PK parameters were estimated. The model selection was based on standard criteria including goodness-of-fit plots, successful outcomes of the estimation and covariance routines, the reasonableness and precision of the parameter estimates, and results of model evaluation using prediction-corrected visual predictive check methodology.[26]

Individual BMS-986166-P exposures on day 1 and day 28 (only for subjects enrolled in Study IM018003) were predicted from the final PPK model using individual maximum a posteriori Bayesian estimates. These exposures served as input for the exposure-response (E-R) models describing HR and ALC responses to BMS-986166-P.

Because the E-R modeling approach applied in our analyses was aimed to mirror the methods described in the clinical pharmacology summary for

fingolimod included in the regulatory review and subsequent marketing approval by the US Food and Drug Administration,[27] the individual subject nadir values for HR and ALC were selected as the response measures to be evaluated in these E-R analyses.

Continuous HR monitoring data were summarized as hourly average HR within each subject and the difference in hourly average HR determined within the same time interval on day –1 and day 1 was individually calculated for each subject. As all subjects received a placebo dose on day –1, this difference was referred to as time-matched placebo-corrected HR (DDHR) where DD ($\Delta\Delta$) refers to the time-matched difference in heart rate between day –1 and day 1, and HR correction for placebo effect. The nadir values of DDHR on day 1 (nDDHR, in beats per minute [bpm]) described the maximum BMS-986166-P effect on HR on day 1, and were used to evaluate the E-R relationship using pooled data from Studies IM018001 and IM018003. Various structural model forms including exponential, inhibitory maximum effect (E_{max}), inhibitory sigmoid E_{max}, and power models were tested to describe the relationship between BMS-986166-P exposure and nDDHR.

Due to the time delay in ALC responses, different magnitudes and times of E_{max} were expected following single and repeated dosing. Therefore, separate E-R models were built for data collected in Studies IM018001 and IM018003 using exposures on day 1 and day 28, respectively. In both models, the nadir value of ALC (nALC, in 10^3 cells/μL) observed at any time following the first BMS-986166 or placebo dose was the metric selected to represent the maximum effect of BMS-986166-P and placebo on ALC following single or repeated dosing. As described above, various structural model forms were also tested to describe the relationship between BMS-986166-P exposures and nALC. An indirect response model was not considered since the direct effect models adequately captured the effect of BMS-986166-P on nALC responses. Subjects randomized to receive placebo treatment on day –1 were included in E-R modeling of nDDHR and nALC and were assumed to be associated with BMS-986166-P exposures of 0.

Interindividual variability (IIV) in PK parameters was assumed to be log-normally distributed and was estimated using exponential variability models. No IIV was estimated in the E-R models. Various residual variability models were tested for the PPK and E-R models, including combinations of additive and constant coefficient of variation models and logarithmic models.

Simulations
Simulations were performed to determine the typical predicted (with uncertainty) BMS-986166-P exposures,

nDDHR on day 1 and nALC following repeated daily doses of 0 mg/day to 5 mg/day of BMS-986166 for 28 days. Each dose regimen was simulated in 1000 virtual subjects assumed to have the characteristics of the subjects in either Study IM018001 or Study IM018003.

Comparison to Other S1P Receptor Modulators
Data on the effects of other S1P receptor modulators on ALC and HR reduction were obtained from published literature. If data were not readily available in text, individual subject results and/or mean profiles of ALC and HR versus time were digitized using the Engauge Digitizer Version 4.1[28] software and processed to calculate the necessary metrics. Effects on HR were compared for doses achieving various degrees of reduction in ALC from baseline (ie, ALC measured at the time of the first dose).

Results
The 62 healthy study participants (30 subjects from Study IM018001 [24 active treatment, 6 placebo] and 32 subjects from Study IM018003 [24 active treatment, 8 placebo]) included in these analyses were mostly male (96.8%) with an average age of 34.7 years (ranging from 19 to 52 years) and weight of 84.2 kg (ranging from 58.3 to 104.1 kg). All subjects had normal renal and hepatic function; 34 subjects were classified as White, 25 as Black or African American, 2 as American Indian or Alaska Native, and 1 as a Native Hawaiian or other Pacific Islander.[29] The demographic characteristics were generally similar for subjects in Study IM018001 and Study IM018003 (Table S2).

A total of 1677 BMS-986166 and 1637 BMS-986166-P concentrations from 48 subjects were used in the PPK analysis, which did not include any concentration below the lower limit of quantification. A total of 61 nDDHR values (1 per subject), including 13 collected in subjects receiving placebo, were included in the E-R analysis of HR on day 1. Baseline ALC and nALC values were included in the E-R analysis data sets: 31 subjects were used in the E-R analysis of nALC after single dosing, including 6 receiving placebo and 1 who received only 1 BMS-986166 dose in Study IM018003; 31 subjects were included in the E-R analysis of nALC after repeated dosing, including 8 subjects receiving placebo.

Population PK Model
Exploratory data analyses (shown in Figure S1) indicated that peak concentrations occur much earlier for BMS-986166-P compared to BMS-986166 (6 hours vs 21 hours and 7.5 hours vs 15 hours in Study IM018001 and Study IM018003, respectively), indicating that BMS-986166 undergoes presystemic transformation into BMS-986166-P during the
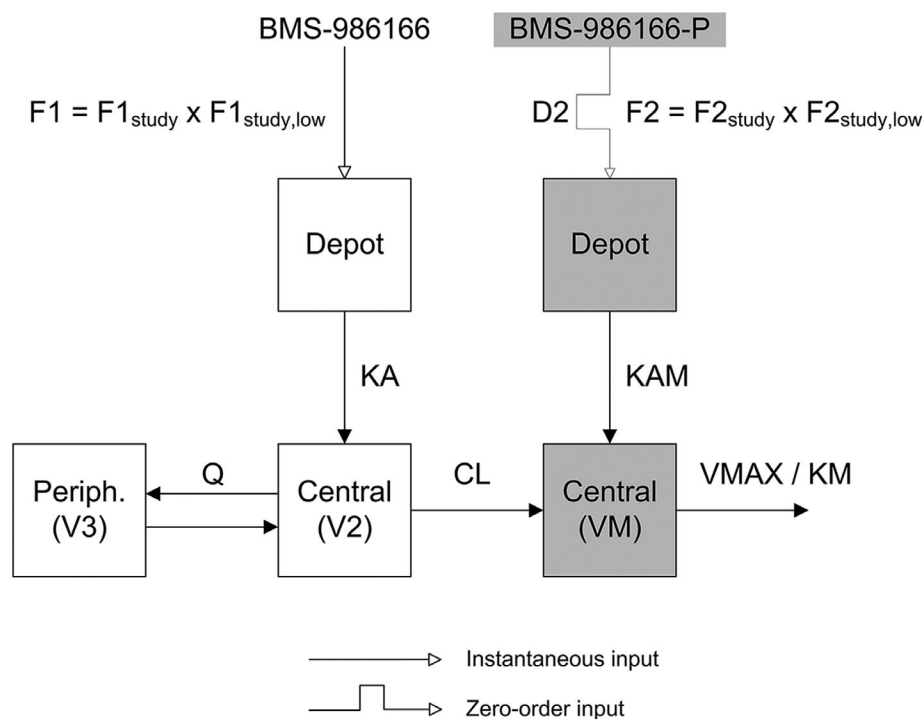
Figure 1. Diagram of the combined model for BMS-986166 and BMS-986166-P pharmacokinetics. CL, apparent elimination clearance for BMS-986166; D2, duration of the zero-order absorption process for BMS-986166-P; $F1_{study}$, relative bioavailability of BMS-986166 in each study; $F1_{study,low}$, proportional shift in F1 in subjects with low exposures in each study; $F2_{study}$, relative bioavailability of BMS-986166-P in each study; $F2_{study,low}$, proportional shift in F2 in subjects with low exposures in each study; KA, first-order rate of absorption for BMS-986166; KAM, first-order rate of absorption for BMS-986166-P; KM, half-inhibitory BMS-986166-P concentration; Q, apparent distribution clearance; V2, apparent central volume for BMS-986166; V3, apparent peripheral volume for BMS-986166; VM, apparent central volume for BMS-986166-P; VMAX, apparent maximum elimination rate for BMS-986166-P.

enteric and/or hepatic first pass. Earlier appearance of BMS-986166-P peak concentrations could result from a combination of faster appearance in the bloodstream, faster elimination, and slower and/or more restricted distribution. Additionally, BMS-986166 PK were dose-proportional over the dose range tested, while BMS-986166-P PK were dose proportional at lower doses, but concentrations appeared to increase in a greater-than-proportional manner after BMS-986166 was administered once-daily for approximately 1 week. Six subjects exhibited lower BMS-986166 and BMS-986166-P exposures compared to the rest of the population, but this observation was not associated with any differences in age, weight, renal or hepatic function biomarkers, or ethnic classification.

Figure 1 shows the structure of the selected combined PK model for BMS-986166 and BMS-986166-P. The base model for BMS-986166 included 2 compartments with first-order absorption, linear distribution and elimination, and study-specific bioavailability. Study-specific shifts in bioavailability were also estimated for subjects identified as having lower exposures. The IIV in the apparent elimination clearance, central volume, and first-order absorption rate constant were also estimated. All parameters were estimated with

good precision (Table 1) and provided a reasonable fit to the data (Figure 2), including accumulation after repeated dosing and elimination after the last dose (Figure 3). Although median peak concentrations were reasonably predicted by the model, individual peak concentrations measured on days 14 and 28 tended to be underpredicted, particularly for the 0.75- and 1.5-mg/day dose groups.

The following assumptions were made to assess the PK of BMS-986166-P in the combined model (Figure 1). These empiric assumptions were implemented for modeling and data description reasons and do not necessarily reflect the actual metabolic pathways of BMS-986166:

- PK of BMS-986166 were fixed to the population mean estimates for fixed and random effect parameters determined for the selected base model.
- BMS-986166 was irreversibly converted into BMS-986166-P.
- Phosphorylation of BMS-986166 into BMS-986166-P was assumed to be the only elimination pathway for BMS-986166.
- Virtual BMS-986166-P doses equal to the molar amounts of BMS-986166 doses times an estimated

Table 1. Parameter Estimates for the Sequential Model of BMS-986166 and BMS-986166-P Pharmacokinetics

Parameter	Final Parameter Estimate		Interindividual Variability/Residual Variability	
	Typical Value	%RSE	Magnitude	%RSE
BMS-986166				
CL: apparent elimination clearance (L/h)	2.51	5.02	34.4 %CV	32.6
V2: apparent central volume (L)	913	3.63	16.8 %CV	20.9
Q: apparent distribution clearance (L/h)	0.763	13.5	NE	NA
V3: apparent peripheral volume (L)	205	11.2	NE	NA
KA: first-order process rate constant (1/h)	0.287	6.65	42.7 %CV	39.8
$F1_{SAD}$: relative bioavailability in Study IM018001 (−)	1.00	FIXED	NE	NA
$F1_{MAD}$: relative bioavailability in Study IM018003 (−)	0.764	4.87	NE	NA
$F1_{SAD,LOW}$: fold change in F1 for subjects with low exposures in Study IM018001 (−)	0.655	5.91	NE	NA
$F1_{MAD,LOW}$: fold change in F1 for subjects with low exposures in Study IM018003 (−)	0.471	13.6	NE	NA
Residual variability for BMS-986166	0.00906	4.75	9.52 %CV	NA
BMS-986166-P				
FM: fraction of CL going to conversion into BMS-986166-P (−)	1.00	FIXED	NE	NA
VMAX: apparent maximum elimination rate for BMS-986166-P (μmol/h)	0.649[a]	19.4	34.1 %CV	32.3
KM: half inhibitory BMS-986166-P concentration (μM)	0.125[a]	19.5	NE	NA
VM: apparent central volume for BMS-986166-P (L)	38.7	7.65	35.1 %CV	32.3
KAM: first-order process rate constant for BMS-986166-P (1/h)	0.382	5.37	26.1 %CV	31.6
D2: zero-order process duration for BMS-986166-P (h)	5.56	1.05	NE	NA
$F2_{SAD}$: fraction absorbed as BMS-986166-P in Study IM018001 (−)	0.0771	7.79	NE	NA
$F2_{MAD}$: fraction absorbed as BMS-986166-P in Study IM018003 (−)	0.0797	7.94	NE	NA
$F2_{SAD,LOW}$: fold change in F2 for subjects with low exposures in Study IM018001 (−)	1.25	16.8	NE	NA
$F2_{MAD,LOW}$: fold change in F2 for subjects with low exposures in Study IM018003 (−)	1.82	22.4	NE	NA
Residual variability for BMS-986166-P	0.0174	8.44	13.2 %CV	NA

%CV, coefficient of variation expressed as a percent; NA, not applicable; NE, not estimated; %RSE, relative standard error (%).
[a] The following parameter estimates were found to be highly correlated ($r^2 \geq 0.810$).

fraction F2 entered the system at the same time as BMS-986166 doses to represent the presystemic transformation of BMS-986166 into BMS-986166-P.

The model component representing the PK of BMS-986166-P was a 1-compartment model with sigmoid absorption (ie, a combination of zero-order input into a depot compartment and first-order transfer from depot to central compartment), saturable elimination, and included a first-order input corresponding to the ratio of BMS-986166 apparent clearance/apparent volume of the central compartment. The data supported the estimation of IIV in the apparent maximum elimination rate of BMS-986166-P, apparent volume, and the first-order rate of the BMS-986166-P absorption process. Although estimates of apparent maximum elimination

rate and the half-maximal inhibitory BMS-986166-P concentration were highly correlated, all parameters were estimated with good precision (Table 1). Similar to the properties of the base model for BMS-986166 PK, the selected combined model was able to reasonably capture the elimination and accumulation of BMS-986166-P (Figures 2 and 3), but underpredicted individual peak concentrations on days 14 and 28. In spite of this, individual area under the concentration curve (and thus, average concentration) after the first and last dose were well predicted by the combined model.

Exposure-Response Analysis: HR
Hourly HR averages and DDHR values exhibited moderate intraindividual variability, but showed that
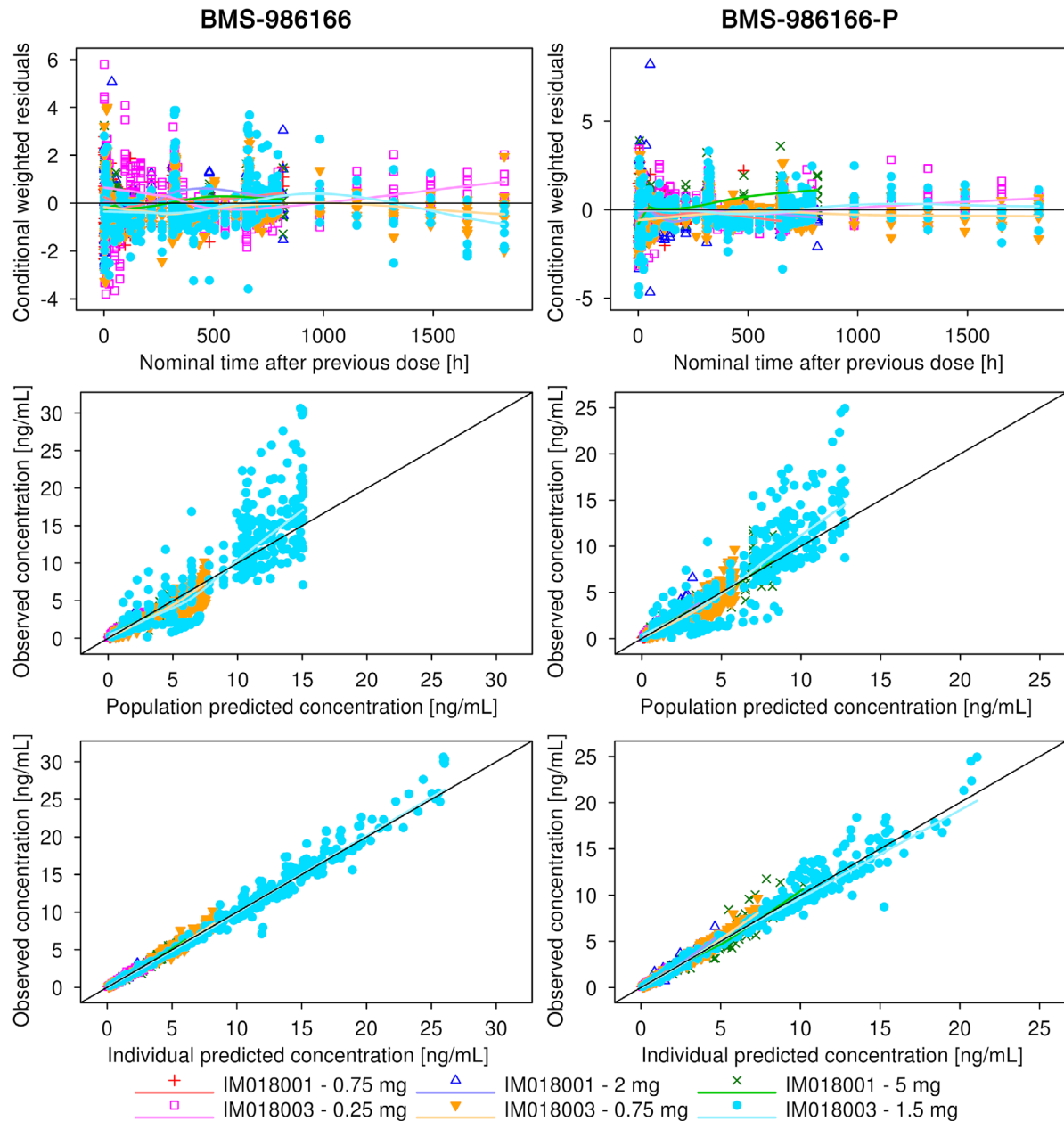
Figure 2. Goodness-of-fit plots for the combined pharmacokinetic model: BMS-986166 (left) and BMS-986166-P (right).

BMS-986166 administration resulted in a dose-dependent decrease in DDHR with no further reduction in HR after repeated dosing (Figure S2). Values for nDDHR ($\sim$–10 bpm) were similar in subjects who received placebo or BMS-986166 0.25 mg. As BMS-986166-P exposure increased, nDDHR decreased and finally reached a plateau at higher BMS-986166-P concentrations. One subject who received placebo exhibited a very low nDDHR value of –40.6 bpm, which was thought to be an outlier. This data point was excluded from the analysis as a conservative measure to avoid underprediction of the magnitude of effect of BMS-986166-P on nDDHR.

An inhibitory sigmoid E_{max} model was selected to describe the relationship between average BMS-986166-P concentrations on day 1 ($C_{avg,Day1}$) and nDDHR:

$$nDDHR = nDDHR_{placebo}$$

$$+ \left(Max\Delta - nDDHR_{placebo}\right) \times \frac{C_{avg,Day1}^{h}}{IC50^{h} + C_{avg,Day1}^{h}}$$

where $nDDHR_{placebo}$ is the nDDHR in subjects receiving placebo; $Max\Delta$ is the maximal reduction in nDDHR; IC50 is the BMS-986166-P concentration at half-maximal response; and h is the Hill coefficient.
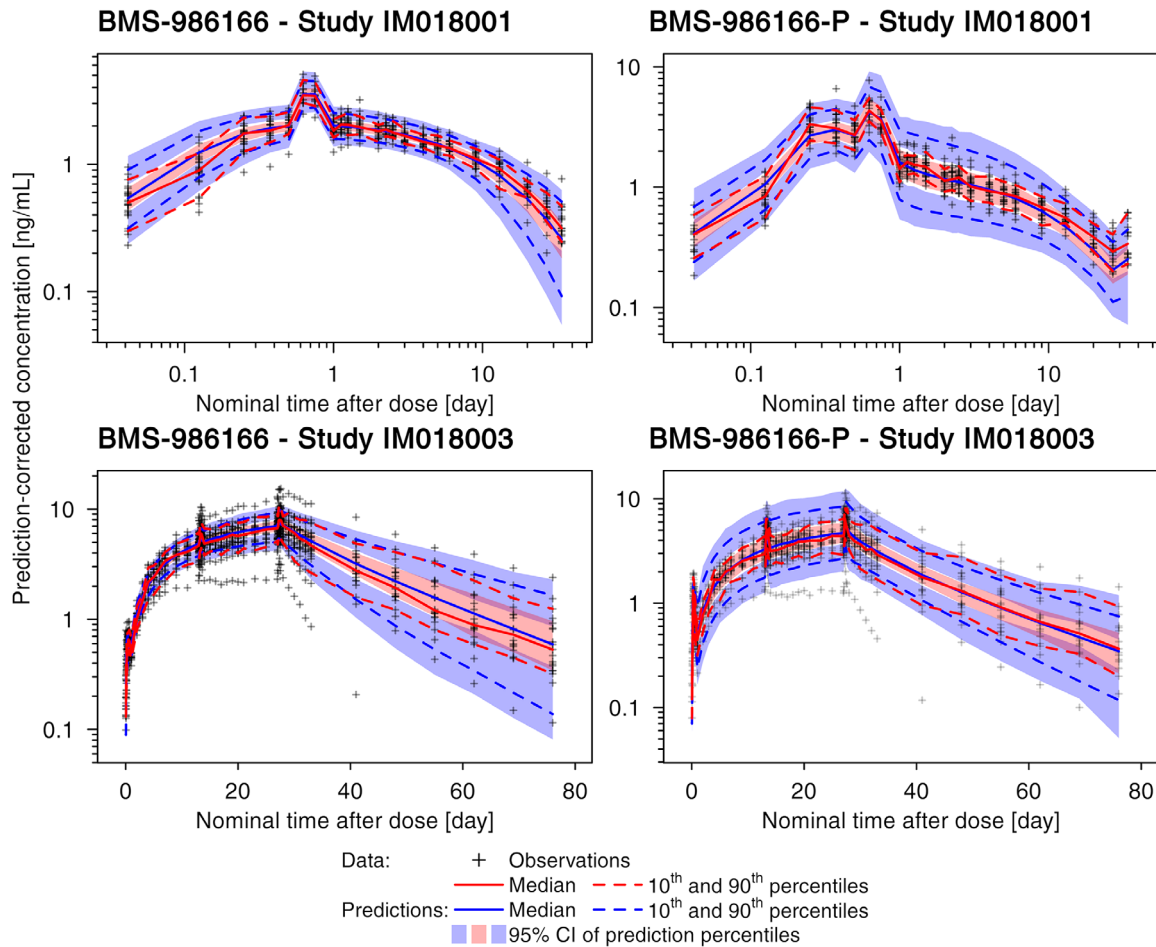
Figure 3. Prediction-corrected visual predictive check plots for the combined pharmacokinetic model: BMS-986166 (left) and BMS-986166-P (right).

Both $nDDHR_{placebo}$ and $Max\Delta$ are negative values. All parameters were estimated with reasonably good precision (Table 2) and provided a good description of the initial decrease and subsequent plateauing of nDDHR as $C_{avg,Day1}$ increases (Figure 4).

Exposure-Response Analysis: Lymphocyte Count
ALCs rapidly declined following BMS-986166 doses (23%-92% change from ALC at time 0 [ALC_0] after multiple doses of 0.25 mg to 1.5 mg/day). Similar nadir values (nALC) were observed in the 0.75 and 1.5 mg/day dose panels after multiple doses, suggesting that a steady-state E_{max} of BMS-986166-P was achieved with a BMS-986166 0.75 mg/day dose regimen. After repeated dosing, ALC tended to remain close to nadir values over the dosing regimen and for longer durations in a dose-dependent manner after the end of the dosing regimen (shown in Figure S3). In contrast, transient fluctuations in ALC were observed following the single or repeated administration of placebo, but on average, the magnitude was similar after single and multiple

doses and resulted in an approximately 20% reduction in ALC compared to ALC_0.

The selected E-R models for nALC after single- and multiple-dose administration estimated the fractional reduction from ALC_0 observed in participants receiving placebo ($\Delta_{placebo}$) and the effect of BMS-986166-P as a fractional reduction relative to nALC predicted for participants receiving placebo. The inhibitory sigmoid E_{max} functions found to best describe the observed data were:

Single dose:
$$nALC = ALC_0 \times \left(1 - \Delta_{placebo}\right)$$
$$\times \left(1 - \frac{Imax \times C_{avg,\ Day1}^{h}}{IC50^h + C_{avg,\ Day1}^{h}}\right)$$

Repeated dosing:
$$nALC = ALC_0 \times \left(1 - \Delta_{placebo}\right)$$
$$\times \left(1 - \frac{Imax \times C_{avg,\ Day28}^{h}}{IC50^h + C_{avg,\ Day28}^{h}}\right)$$

where I_{max} is the maximum fractional reduction in nALC due to BMS-986166-P; and $C_{avg,\ Day28}$

Table 2. Parameter Estimates for the Exposure-Response Models for Nadir Placebo-Corrected Heart Rate and Nadir Absolute Lymphocyte Counts

Parameter	Final Parameter Estimate		Interindividual Variability/Residual Variability	
	Typical Value	%RSE	Magnitude	%RSE
nDDHR				
$nDDHR_{placebo}$: nDDHR in participants receiving placebo (bpm)	−9.08	10.8	NE	NA
$Max\Delta$: maximum reduction in nDDHR (bpm)	−19.7	10.9	NE	NA
IC50: $C_{avg,Day1}$ at half-maximal response (ng/mL)	1.26	40.1	NE	NA
h: Hill coefficient	1.84	33.2	NE	NA
Residual variability	0.167	19.1	40.9 %CV	NA
nALC after single dose				
ALC_0: baseline nALC (10^3 cells/µL)	2.061	6.257	NE	NA
I_{max}: fractional reduction in nALC relative to placebo[a]	0.6747	20.59	NE	NA
IC50: $C_{avg,Day1}$ at half-maximal response (ng/mL)	2.693	13.65	NE	NA
h: Hill coefficient[a]	3.080	76.98	NE	NA
$\Delta_{placebo}$: fractional reduction in nALC in participants receiving placebo	0.1992	29.20	NE	NA
Residual variability	0.08569	29.10	29.27 %CV	NA
nALC after repeated dosing				
ALC_0: baseline nALC (10^3 cells/µL)	1.95	5.55	NE	NA
I_{max}: fractional reduction in nALC relative to placebo	0.768	9.26	NE	NA
IC50: $C_{avg,Day28}$ at half-maximal response (ng/mL)	1.72	23.9	NE	NA
h: Hill coefficient	1.65	44.8	NE	NA
$\Delta_{placebo}$: fractional reduction in nALC in participants receiving placebo	0.284	29.4	NE	NA
Residual variability	0.0880	18.0	29.7 %CV	NA

ALC_0, absolute lymphocyte count at time 0; %CV, coefficient of variation expressed as a percentage; NA, not applicable; nALC, nadir of absolute lymphocyte count; nDDHR, nadir of time-matched placebo-corrected heart rate; NE, not estimated; %RSE, relative standard error (%).
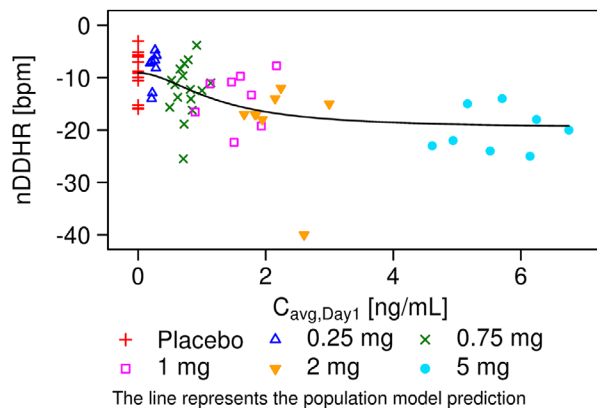[a] The following parameter estimates were found to be highly correlated ($r^2 \geq 0.8100$).

Figure 4. Observed and model-predicted nadir time-matched placebo-corrected heart rate on day 1 vs model-predicted average BMS-986166-P concentration on day 1

is the average BMS-986166-P concentration on day 28.

The parameter estimates for the nALC models after a single dose and repeated dosing were generally well estimated, except for the Hill coefficients (Table 2).

The relative standard error (%) values for the estimated Hill coefficients were 76.98 and 44.8, respectively, for the nALC after single and repeated doses. Mean model predictions described the decrease and plateauing of nALC as BMS-986166-P exposure increased (Figure 5).

Simulations

Using the final combined PPK and E-R models, the typical values of BMS-986166-P exposures ($C_{avg,\ Day1}$ and $C_{avg,\ Day28}$) and associated nDDHR and nALC responses were predicted (with uncertainty) for various daily dosing regimens ranging from 0 mg/day to 5 mg/day. The typical predicted nDDHR and nALC for subjects considered to have normal or low (based on visual inspection) exposures are represented in Figure 6 as a change and a percent change from placebo response (with 90% confidence interval). The results suggest that multiple-dose regimens between 0.75 mg/day and 2 mg/day would achieve a 65% reduction in ALC compared to placebo, but a 75% reduction of ALC compared to baseline (defined as
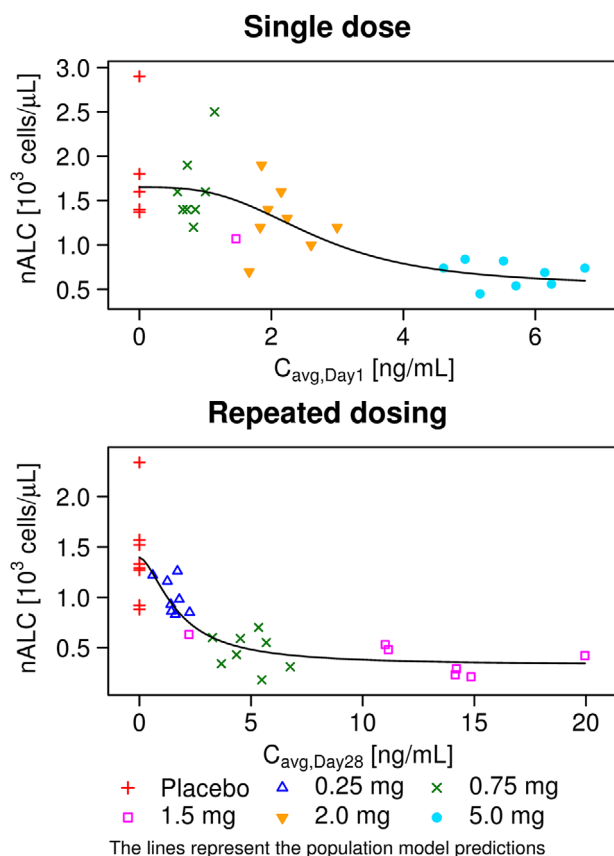
Figure 5. Observed and model-predicted nadir absolute lymphocyte counts versus average BMS-986166-P concentration on day 1 or day 28 after single dose (top) and repeated dosing (bottom).

Figure 6. Model-predicted change in nadir time-matched placebo-corrected heart rate on day 1 and nadir absolute lymphocyte counts relative to placebo response versus BMS-986166 dose in subjects with normal exposures (top) and low exposures (bottom) at steady state. The shaded areas represent the 90% confidence intervals around the median lines. The dashed blue line represents a drop of 8 bpm in nDDHR compared to placebo. The horizontal dashed red line represents a drop of 65% in nALC compared to placebo. nALC, nadir of absolute lymphocyte count; nDDHR, nadir of time-matched placebo-corrected heart rate.

the ALC at the time of the first dose) in subjects with normal exposures (top panel) and result in a maximum reduction in nDDHR relative to placebo of –8 bpm. For subjects with low exposures (bottom panel), doses that achieve the same targets fall between 1 mg/day and 1.75 mg/day. However, this result should be interpreted with caution as these low exposures are estimated with less certainty. The downward shifts in bioavailability that drive the difference in effects on HR and ALC reduction in the subjects with low exposures were estimated on a limited number of subjects (ie, only 6 subjects who contributed to the E-R model of nDDHR and 2 who contributed to the E-R model of nALC).

Discussion

A combined model was developed to describe the PK of BMS-986166 and BMS-986166-P following single and repeated dosing of BMS-986166 in healthy participants. The model provided a reasonable fit to the data overall but generally underpredicted peak concentrations of both compounds measured on days 14 and 28. Exploratory data analyses showed that
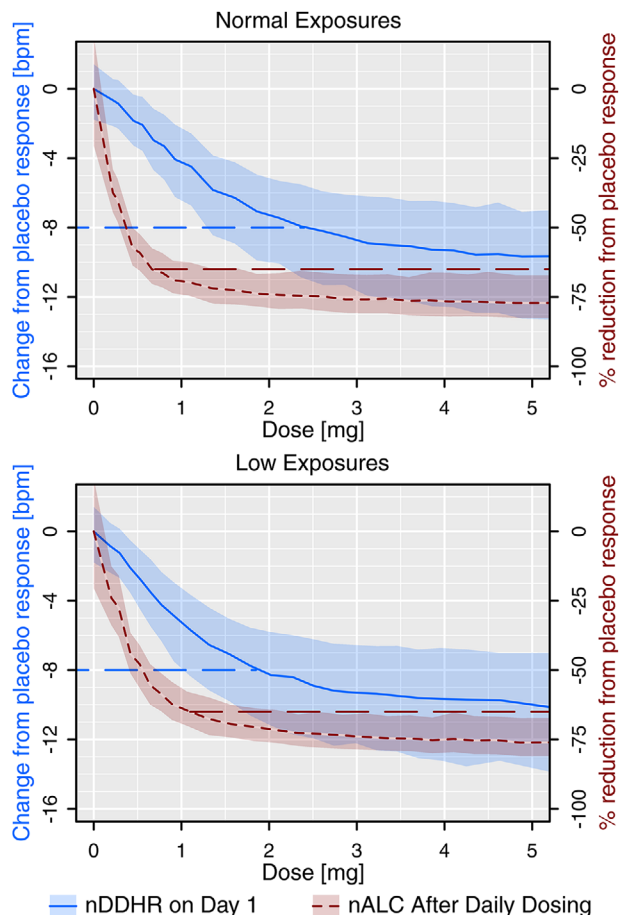
peak-to-trough concentration ranges for BMS-986166 and BMS-986166-P tended to increase over time, while the opposite pattern is typically observed due to drug accumulation in compounds with linear or nonlinear PK. Other models were tested for both BMS-986166 and BMS-986166-P to capture these time-dependent trends. However, models including saturable elimination (BMS-986166), distribution, or binding in the central or peripheral compartments, time-dependent bioavailability, absorption rate, or disposition either did not minimize successfully with a covariance step or did not significantly improve the model performance with respect to the prediction of peak concentrations.

Because the PK of BMS-986166 cannot practically be evaluated after intravenous administration and

BMS-986166-P cannot be directly administered, it was not possible to simultaneously estimate parameters describing BMS-986166 and BMS-986166-P PK or develop a more mechanistic and physiologically representative model as was done for fingolimod.[30] In particular, the relative fractional conversion of BMS-986166 to BMS-986166-P occurring presystemically (eg, in the gastrointestinal tract) vs that occurring after absorption (eg, in the liver) was not identifiable based on the available data. Furthermore, it was necessary to assume in the model that the conversion of BMS-986166 to BMS-986166-P was unidirectional due to similar parameter identifiability issues.

Several empiric components were included in the selected combined model. First, the relative bioavailability (F) of BMS-986166 in Study IM018003 compared to Study IM018001 was estimated. For purposes of obtaining this estimation of F, the bioavailability of Study IM0181001 was assumed to be 1 to serve as the reference. The inclusion of this parameter significantly improved the objective function and data fit, but may just represent a compensation for time-dependent changes in the PK after repeated dosing in Study IM018003 in the model, rather than an actual difference in bioavailability. Second, the presystemic formation and absorption of BMS-986166-P was represented by the administration of a virtual dose of BMS-986166-P. When taken in combination with the assumption of complete conversion of BMS-986166 to BMS-986166-P, administration of this virtual dose meant that more molar units of BMS-986166-P entered the model than was actually administered as BMS-986166. Therefore, all BMS-986166-P parameters should be considered as apparent and relative to this extra amount of drug. In the absence of BMS-986166 and BMS-986166-P concentration data obtained after the administration of BMS-098266-P, inclusion of this model feature was necessary to capture the occurrence of BMS-986166-P peak concentrations before the occurrence of BMS-986166 peak concentrations. Finally, study-specific shifts in BMS-986166 and BMS-986166-P relative bioavailability were estimated for 12.5% of the study population who were identified to have lower exposures for both entities. No significant difference in subject characteristics was found between the 2 subpopulations. Therefore, it is unclear what factors contribute to this phenomenon. However, the estimates of the bioavailability shifts for BMS-986166 (<1) and BMS-986166-P (>1) suggested that subjects determined to have lower drug exposures may also experience higher presystemic conversion of BMS-986166 to BMS-986166-P.

No further reduction of HR was observed beyond day 1 following repeated dosing with BMS-986166.

This finding contrasted with the further reduction in HR reported following repeated dosing with GSK2018682,[13] or the delayed HR decrease following amiselimod dosing,[9,10] but was consistent with similar observations for fingolimod,[5,13] cenerimod,[11] ponesimod,[15,16] and siponimod.[17,18] The transient reduction in HR following fingolimod dosing was linked to fingolimod initially acting as a full S1PR agonist and thereafter functioning as an S1PR antagonist with downregulation of S1P1R, as the continuous exposure to fingolimod results in the internalization of the drug-receptor complexes and reduction in the numbers of S1P1R present on the cell surface.[8] A direct-effect I_{max} PK/PD model based on data from 9 clinical studies was developed for ponesimod that included a component for tolerance development to describe this transient reduction in HR with treatment initiation that disappears following repeated dosing.[31] Given the lack of continued reduction in HR following repeated once-daily doses of BMS-986166, the data collected on day 1 were used to quantify the relationship between BMS-986166-P exposures and nDDHR.

Given the underprediction of peak BMS-986166-P concentrations by the selected model despite adequate description of daily exposures and average concentrations of BMS-986166-P, coupled with a high correlation between maximum and average observed BMS-986166-P concentrations on day 1 or day 28 (r = 0.98224 and r = 0.99845, respectively), model-predicted average concentrations were used for E-R modeling and simulations.

Both models included parameters to estimate the magnitudes of change in nDDHR or nALC in participants who were randomized to placebo treatment. These estimates should not be interpreted as placebo effects, as the dynamics of HR and ALC have been previously shown to exhibit circadian rhythms.[32,33] For the ALC model, $\Delta_{placebo}$ reflected the portion of the circadian cycle where ALC was physiologically lower and captured the maximum decrease in ALC compared to ALC_0. The nDDHR metric was based on time-matched correction which should have eliminated the changes in HR due to circadian rhythm. However, because HR varied slightly from day to day within participants, DDHR was not constant on day 1. Therefore, $nDDHR_{placebo}$ reflected the maximum difference in HR between day 1 and day –1 due to intrasubject variability in participants receiving placebo.

The selected inhibitory sigmoid E_{max} model accurately described the E-R relationship for nDDHR, where a $nDDHR_{placebo}$ of –9.1 bpm and a maximal HR reduction due to drug effect of 10.6 bpm was achieved at an average BMS-986166-P concentration of approximately 4 ng/mL (Table 2), resulting in a combined reduction of 19.7 bpm in nDDHR.

Similarly, inhibitory sigmoid E_{max} models were selected to describe the E-R relationship for nALC after single and repeated dosing. Both models recaptured the data well and were defined by generally well-estimated parameters. In the single-dose model for nALC, however, the precision of the Hill coefficient was not precisely estimated and was highly correlated with the estimate of I_{max}, most likely due to the paucity of data in the decreasing portion of the sigmoid curve in the relationship between nALC and $C_{avg, \, Day1}$. In comparison, the model that best described the relationship between cenerimod concentration and lymphocyte count in healthy subjects (4 phase 1 studies) and patients with systemic lupus erythematosus (1 phase 2 study) was composed of a circadian rhythm, a lymphocyte count compartment, and a drug effect modeled with a saturable inhibitory (I_{max}) function. An indirect response model was used to describe the drug effect on lymphocyte count. Similar models were previously used to describe the effect of ponesimod on lymphocyte count[34,35] and lymphocyte subsets.[35]

Estimates of $\Delta_{placebo}$ were slightly higher in the repeated-dose model compared to the single-dose model (Table 2). While the average observed ALC_0 values were similar across all subjects in Studies IM018001 and IM018003 (approximately 2.00×10^3 cells/µL), lower ALC_0 (1.76×10^3 cells/µL vs 2.25×10^3 cells/µL) and nALC values (1.39×10^3 cells/µL vs 1.70×10^3 cells/µL) were observed in subjects receiving placebo in Study IM018003 compared to those receiving placebo in Study IM018001. As only a small number of subjects received placebo in each study and because $\Delta_{placebo}$ was expressed as a relative change from ALC_0 estimated across subjects who received BMS-986166 or placebo, the difference in $\Delta_{placebo}$ estimates was most likely the result of selection bias. Based on the estimated I_{max}, the level of ALC reduction for BMS-986166 was similar to that of other S1P receptor modulators (Table S3) and was only slightly lower in the single-dose model compared to the repeated-dose model (Table 2).

Simulations predicted that a 65% reduction in ALC from baseline can typically be achieved at $C_{avg, \, Day28}$ of 3.5 ng/mL, which typically corresponds to a BMS-986166 dose of 0.5 mg/day. At this dose, a typical reduction in nDDHR on day 1 is predicted to be 11.0 bpm compared to a 9.1-bpm reduction for subjects who would receive placebo, a difference of approximately 2 bpm attributable to BMS-986166. To contrast the magnitude of these effects, data on the changes in HR and ALC following administration of other S1P receptor modulators, including amiselimod, cenerimod, ceralifimod, fingolimod, GSK2018682, ozanimod, ponesimod, and siponimod, were extracted from the literature (Table S3). Our comparison focused on reports of changes in HR and ALC following

fixed-dose administration at regimens that produced significant reductions in ALC compared to placebo. For HR, only the data collected on day 1 were considered. Supporting studies were generally placebo-controlled trials conducted in healthy participants (if not mentioned otherwise in Table S3) with intensively measured HR and ALC. Some of these studies implemented a protocol that did not include measurements of HR and ALC after administration of placebo on the day before the initiation of treatment with the active drug or placebo. Therefore, it was not always possible to calculate nDDHR as done in our analyses. In such cases, the HR effect was calculated as the minimum of the baseline-corrected HR following the first dose of active drug or placebo. This metric assumes a time-invariant correction, while nDDHR implements a time-varying correction using measured day –1 data.

For ponesimod, only the mean of baseline-corrected HR following the first dose of active drug or placebo was available. The maximum HR effect of the active treatment relative to placebo at doses producing approximately 70% reduction in ALC varied across molecules and ranged from approximately –21 to –6.5 bpm for siponimod,[17,18] from –18 to –12 bpm for ponesimod,[15,16] –11 to –6 bpm for fingolimod,[12,30] from –14 to –13 bpm for GSK2018682,[13] and from –8 to –6 bpm for ozanimod.[14] Ceralifimod provided only 56% reduction in ALC at the highest reported dosage (ie, 0.1 mg/day) and induced up to –8 bpm HR effect over placebo.[12] The maximum reduction in ALC achieved with cenerimod was approximately 64% and was associated with <1-bpm HR effect over placebo.[11] Amiselimod was reported to induce delayed effect on HR with no significant[10] or small (ie, <–4-bpm reduction[10]) influence observed following the first administration of doses reducing ALC by approximately 70%. However, HR reductions between –8 and –10 bpm were reported by day 7 for amiselimod.

Overall, it appears that BMS-986166 has lower HR liability while maintaining similar efficacy compared to most S1P receptor modulators following fixed-dosing regimens. At the dose level predicted to be therapeutic, a requirement for clinical monitoring is not anticipated. Nevertheless, given the steepness of the E-R relationship for nALC at low doses, a titration schedule is under consideration to assess any further improvement in the safety profile of BMS-986166, as was proposed for other S1P receptor modulators.[14,36–39]

Conclusion

A fit-for-purpose joint model was successfully developed to jointly quantify the PK of BMS-986166 and its active metabolite BMS-986166-P after single and repeated dosing in healthy participants. Inhibitory

sigmoid E_{max} models described the relationships between model-predicted average BMS-986166-P concentrations and observed nDDHR and nALC (ie, the minimum value of time-matched placebo-corrected HR and the minimum value of ALC). Based on the PK/PD model, a 0.5-mg/day dose of BMS-986166 was predicted to achieve 65% reduction in ALC associated with a 2-bpm decrease in nDDHR over placebo.

Conflicts of Interest

S.S., D.S., H.S., J.X., S.B., A.L., S.D., A.F., J.T., and I.G. are or were employees and/or shareholders of Bristol Myers Squibb, which sponsors the development of BMS-986166. S.B., E.L., H.H., and K.L. are or were employees of Cognigen Corporation, which was contracted by Bristol Myers Squibb to perform the analyses reported in this article.

References

1. Hla T. Physiological and pathological actions of sphingosine-1-phosphate. *Semin Cell Dev Biol*. 2004;15: 513-520.
2. Gilmore JL, Xiao HY, Dhar TGM, et al. Identification and preclinical pharmacology of ((1 R,3 S)-1-amino-3-((S)-6-(2-methoxyphenethyl)-5,6,7,8-tetrahydronaphthalen-2-yl)cyclopentyl)methanol (BMS-986166): a differentiated sphingosine-1-phosphate receptor 1 (S1P1) modulator advanced into clinical trials. *J Med Chem*. 2019;62(5):2265-2285.
3. Dyckman A. Modulators of sphingosine-1-phosphate pathway biology: recent advances of sphingosine-1-phosphate receptor 1 (S1P1) agonists and future perspectives. *J Med Chem*. 2017;60(13):5267-5289.
4. Chaudhry BZ, Cohen JA, Conway DS. Sphingosine 1-phosphate receptor modulators for the treatment of multiple sclerosis. *Neurotherapeutics*. 2017;14(4):859-873.
5. Huwiler A, Zangemeister-Wittke U. The sphingosine 1-phosphate receptor modulator fingolimod as a therapeutic agent: recent findings and new perspectives. *Pharmacol Ther*. 2018;185:34-49.
6. Cohen JA, Barkhof F, Comi G, et al. Oral fingolimod or intramuscular interferon for relapsing multiple sclerosis. *N Engl J Med*. 2010;362:402-415.
7. Subei AM, Cohen JA. Sphingosine 1-phosphate receptor modulators in multiple sclerosis. *CNS Drugs*. 2015;29(7):565-575.
8. Camm J, Hla T, Bakshi R, Brinkmann V. Cardiac and vascular effects of fingolimod: mechanistic basis and clinical implications. *Am Heart J*. 2014;168(5):632-644.
9. Sugahara K, Maeda Y, Shimano K, et al. Amiselimod, a novel sphingosine 1-phosphate receptor-1 modulator, has potent therapeutic efficacy for autoimmune diseases, with low bradycardia risk. *Br J Pharmacol*. 2017;174(1):15-27.
10. Harada T, Wilbraham D, de La Borderie G, Inoue S, Bush J, Camm AJ. Cardiac effects of amiselimod compared with fingolimod and placebo: results of a randomised, parallel-group, phase I study in healthy subjects. *Br J Clin Pharmacol*. 2017;83(5):1011-1027.
11. Juif PE, Baldoni D, Reyes M, et al. Pharmacokinetics, pharmacodynamics, tolerability, and food effect of cenerimod, a selective S1P1 receptor modulator in healthy subjects. *Int J Mol Sci*. 2017;18(12):2636.
12. Krösser S, Wolna P, Fischer TZ, et al. Effect of ceralifimod (ONO-4641) on lymphocytes and cardiac function: randomized, double-blind, placebo-controlled trial with an open-label fingolimod arm. *J Clin Pharmacol*. 2015;55(9):1051-1060.
13. Xu J, Gray F, Henderson A, et al. Safety, pharmacokinetics, pharmacodynamics, and bioavailability of GSK2018682, a sphingosine-1-phosphate receptor modulator, in healthy volunteers. *Clin Pharmacol Drug Dev*. 2014;3(3):170-178.
14. Tran JQ, Hartung JP, Peach RJ, et al. Results from the first-in-human study with ozanimod, a novel, selective sphingosine-1-phosphate receptor modulator. *J Clin Pharmacol*. 2017;57(8):988-996.
15. Brossard P, Scherz M, Halabi A, Maatouk H, Krause A, Dingemanse J. Multiple-dose tolerability, pharmacokinetics, and pharmacodynamics of ponesimod, an S1P1 receptor modulator: favorable impact of dose uptitration. *J Clin Pharmacol*. 2014;54(2):179-188.
16. Brossard P, Derendorf H, Xu J, Maatouk H, Halabi A, Dingemanse J. Pharmacokinetics and pharmacodynamics of ponesimod, a selective S1P1 receptor modulator, in the first-in-human study. *Br J Clin Pharmacol*. 2013;76(6):888-896.
17. Gergely P, Nuesslein-Hildesheim B, Guerini D, et al. The selective sphingosine 1-phosphate receptor modulator BAF312 redirects lymphocyte distribution and has species-specific effects on heart rate. *Br J Pharmacol*. 2012;167(5):1035-1047.
18. Legangneux E, Gardin A, Johns D. Dose titration of BAF312 attenuates the initial heart rate reducing effect

in healthy subjects. *Br J Clin Pharmacol*. 2013;75(3):831-841.

19. Singhal S, Girgis IG, Xie J, Dutta S, Shevaell DE, Throup J. The safety and pharmacokinetics of a novel, selective S1P1R modulator in healthy participants. *Exp Opin Invest Drugs*. 2020;29:411-22.

20. ClinicalTrials.gov. Identifier NCT02790125. A randomized, double blind placebo-controlled, single ascending dose study to evaluate the safety, tolerability, pharmacokinetics, and pharmacodynamics of BMS-986166 in healthy subjects. https://clinicaltrials.gov/ct2/show/NCT02790125. Published November 24, 2017. Accessed September 18, 2020.

21. ClinicalTrials.gov. Identifier NCT03038711. A multiple dose study to assess the safety and tolerability of BMS-986166 in healthy volunteers. https://clinicaltrials.gov/ct2/show/NCT03038711. Published August 31, 2017. Accessed September 18, 2020.

22. Beal SL, Sheiner LB, Boeckmann AJ, Bauer RJ. NONMEM User's Guides. Ellicott City, MD: ICON Development Solutions; 1989 to 2014.

23. Bihorel S, Fox D, Phillips L, Grasela T. KIWI: a collaborative platform for modeling and simulation. Poster presented at: Annual Meeting of the Population Approach Group in Europe (PAGE); June 10-13, 2014; Alicante, Spain.

24. SAS [computer program]. Version 9.4. Cary, NC: SAS Institute Inc.; 2013.

25. Lindbom L, Pihlgren P, Jonsson EN. PsN-Toolkit—a collection of computer intensive statistical methods for non-linear mixed effect modeling using NONMEM. *Comput Methods Programs Biomed*. 2004;79:241-257.

26. Bergstrand M, Hooker AC, Wallin JE, Karlsson MO. Prediction-corrected visual predictive checks for diagnosing nonlinear mixed-effects models. *AAPS J*. 2011;13:143-151.

27. Drugs@FDA. Application Number 22-527. Clinical pharmacology and biopharmaceutics review(s). https://www.accessdata.fda.gov/drugsatfda_docs/nda/2010/022527Orig1s000clinpharmr.pdf. Published November 12, 2010. Accessed August 13, 2018.

28. Mitchell M. Engauge Digitizer. Version 4.1. https://markummitchell.github.io/engauge-digitizer/. Published 2002. Accessed September 18, 2020.

29. United States Food and Drug Administration. Guidance for industry and food and drug administration staff: collection of race and ethnicity data in clinical trials. https://www.fda.gov/downloads/regulatoryinformation/guidances/ucm126396.pdf. Published October 2016. Accessed September 18, 2020.

30. Snelder N, Ploeger BA, Luttringer O, Stanski DR, Danhof M. Translational pharmacokinetic modeling of fingolimod (FTY720) as a paradigm compound subject to sphingosine kinase-mediated phosphorylation. *Drug Metab Dispos*. 2014;42(9):1367-1378.

31. Lott D, Lehr T, Dingemanse J, Krause A. Modeling tolerance development for the effect on heart rate of the selective S1P1 receptor modulator ponesimod. *Clin Pharmacol Ther*. 2018;103(6):1083-1092.

32. Guo YF, Stein PK. Circadian rhythm in the cardiovascular system: chronocardiology. *Am Heart J*. 2003;145:779-786.

33. Druzd D, Matveeva O, Ince L, et al. Lymphocyte circadian clocks control lymph node trafficking and adaptive immune responses. *Immunity*. 2017;46:120-132.

34. Krause A, Brossard P, D'Ambrosio D, Dingemanse J. Population pharmacokinetics and pharmacodynamics of ponesimod, a selective S1P1 receptor modulator. *J Pharmacokinet Pharmacodyn*. 2014;41:261-278.

35. Lott D, Krause A, Seemayer CA, Strasser DS, Dingemanse J, Lehr T. Modeling the effect of the selective S1P1 receptor modulator ponesimod on subsets of blood lymphocytes. *Pharm Res*. 2017;34:599-609.

36. Kappos L, Li DK, Stuve O, et al. Safety and efficacy of siponimod (BAF312) in patients with relapsing-remitting multiple sclerosis: dose-blinded, randomized extension of the phase 2 BOLD study. *JAMA Neurol*. 2016;73:1089-1098.

37. Scherz MW, Brossard P, D'Ambrosio D, Ipek M, Dingemanse J. Three different up-titration regimens of ponesimod, a selective S1P1 receptor modulator, in healthy subjects. *J Clin Pharmacol*. 2015;55:688-697.

38. Cohen JA, Arnold DL, Comi G, et al. Safety and efficacy of the selective sphingosine 1-phosphate receptor modulator ozanimod in relapsing multiple sclerosis (RADIANCE): a randomised, placebo-controlled, phase 2 trial. *Lancet Neurol*. 2016;15(4):373-381.

39. Hoch M, D'Ambrosio D, Wilbraham D, Brossard P, Dingemanse J. Clinical pharmacology of ponesimod, a selective S1P1 receptor modulator, after uptitration to supratherapeutic doses in healthy subjects. *Eur J Pharm Sci*. 2014;63:147-153.

Supplemental Information

Additional supplemental information can be found by clicking the Supplements link in the PDF toolbar or the Supplemental Information section at the end of web-based version of this article.